Soft-X-Ray Coherent Radiation Using a Single-Cascade Free-Electron Laser

E. Allaria and G. De Ninno
Sincrotrone Trieste, 34012 Trieste, Italy
(Received 2 December 2006; published 5 July 2007)

Coherent harmonic generation using single-pass free-electron lasers is a promising method for generating coherent radiation in the vacuum ultraviolet and x-ray spectral region. We propose a simple scheme allowing one to generate powerful coherent radiation in the soft x-ray region by making use of present available technology. The method relies on the possibility of creating substantial bunching in a relativistic electron beam, while limiting the growth of its energy spread. The validity of the scheme is demonstrated using a simple one-dimensional model. Results are confirmed by three-dimensional simulations.

DOI: 10.1103/PhysRevLett.99.014801 PACS numbers: 41.60.Cr

Free-electron lasers (FEL's) are sources of coherent and powerful radiation potentially operating in the spectral range from the infrared to hard x rays. In particular, the ambitious goal of obtaining laser light in x-ray wavelength region rests on the successful evolution of single-pass FEL configurations. Many proposals and several funded projects exist to build such shorter wavelength sources worldwide [1]. Realization of these sources will provide great opportunities by opening up more detailed investigations of many new areas of science [2]. Among single-pass FEL's, two different schemes can be distinguished, depending on the origin of the optical wave which is used to initiate the process. In the self-amplified spontaneous emission (SASE) configuration [3], the initial seed is provided by the spontaneous emission of the electron beam. SASE-based devices produce tunable radiation at short (x-ray) wavelengths with several gigawatt (GW) peak power, excellent spatial mode, but rather poor temporal and spectral coherence. Recently, new ideas have been proposed to produce fully coherent hard x-ray SASE pulses, see, e.g., [4]. An alternate approach to SASE is coherent harmonic generation (CHG), which is capable of producing temporally and spectrally coherent pulses [5–12]. The standard process leading to CHG is based on the up-frequency conversion of a high-power seeding signal. The classical scheme for CHG has been proposed in [7,8] and successfully utilized at Brookhaven to produce coherent radiation in the infrared [11] and UV [12] spectral region. Such a scheme is characterized by a limited wavelength conversion efficiency and, as a consequence, does not allow a straightforward extension of the spectral range towards x rays. For this reason, the conceptual designs of future vacuum ultraviolet (VUV)/x-ray light sources relying on CHG are based on more complicated configurations [13,14]. In this Letter, we propose a simple method allowing to reach the soft x-ray spectral region by means of a compact and easy-to-implement scheme. Such a method, which is based on a simple modification of the classical scheme proposed in [8], assures a significant improvement of the wavelength conversion efficiency. Moreover, the output radiation is expected to show a better spectral quality than that obtained using presently proposed configurations. In the following, the validity of the method we propose is first demonstrated in the framework of a well known [15] 1D theoretical model which, although very simple, captures the main features of the dynamics of a single-pass FEL. Then, results are tested and confirmed by means of the 3D numerical code GENESIS [16]. By putting forward the hypothesis of one-dimensional (longitudinal) motion and monochromatic radiation, the steady-state dynamics of a single-pass FEL is described by the following set of equations:

$$\frac{d\theta_j}{d\bar{z}} = p_j, \tag{1}$$

$$\frac{dp_j}{d\bar{z}} = -Ae^{i\theta_j} - A^* e^{-i\theta_j}, \tag{2}$$

$$\frac{dA}{d\bar{z}} = \frac{1}{N}\sum_j e^{-i\theta_j}, \tag{3}$$

where $\bar{z} = 2k_u\rho z\gamma_r^2/\langle\gamma_0\rangle^2$ is the rescaled longitudinal coordinate, which plays the role of time. Here, $\rho = (a_w\omega_p/4ck_u)^{2/3}/\gamma_r$ is the so-called Pierce parameter, γ_r the resonant energy, $\langle\gamma\rangle_0$ the mean energy of the electrons at the undulator entrance, k_u the wave vector of the undulator, $\omega_p = (e^2\bar{n}/m\varepsilon_0)^{1/2}$ the plasma frequency, $\bar{n}$ being the electron number density, c the speed of light, ε_0 the permittivity of free space, e and m, respectively, the charge and mass of the electron. Further, $a_w = eB_w/(k_u mc^2)$, where B_w is the rms undulator field. Introducing the wave number $k = 2\pi/\lambda$ of the FEL radiation (λ being the laser wavelength), the phase θ is defined by $\theta = (k + k_u)z - \omega t$ (where $\omega = 2\pi c/\lambda$); its conjugate momentum reads $p = (\gamma - \langle\gamma\rangle_0)/(\rho\langle\gamma\rangle_0)$. The complex amplitude $A = A_x + iA_y$ represents the scaled field, perpendicular to z. The intensity I and the phase φ of the wave are defined by $A = \sqrt{I/N}\exp(-i\varphi)$ (N being the number of electrons). Here $(p_j,\ \theta_j)$ for $1 \le j \le N$ and $(I,\ \varphi)$ are canonically conjugated variables. A key parameter is the electron bunching, which is defined as $b(\bar{z}) = \sum \exp[i\theta_i(\bar{z})]/N := \langle\exp[i\theta(\bar{z})]\rangle$. The latter provides a

quantitative measure of the degree of spatial compactness of the electron distribution.

In the classical approach to CHG [8] the seed and the electron beam interact in a short undulator, called modulator, tuned at the seed wavelength λ. The interaction leads to a modulation of electrons' energy, $\Delta\gamma$. Such a modulation is then converted into a spatial microbunching as the beam transverses a dispersive section (e.g., a magnetic chicane). A spectral analysis of the beam density at the end of the dispersive section shows significant bunching at the seed wavelength and some of its harmonics, i.e., $\lambda/2, \ldots, \lambda/m$. Finally, when injected into a second undulator, called radiator and tuned at the nth harmonic (with $n \leq m$) of the seed wavelength, the microbunched electron beam emits coherent radiation at the harmonic wavelength λ/n. The bunching at different harmonics can be calculated according to the following relation [8]:

$$b_m = \exp(-\tfrac{1}{2}m^2\sigma_\gamma^2 D^2) J_m(m\Delta\gamma D), \tag{4}$$

where $\sigma_\gamma \equiv \langle\gamma - \langle\gamma\rangle\rangle_0$ is the electron-beam incoherent energy spread at the modulator entrance, $D = (2\pi R_{56})/(\lambda\langle\gamma\rangle_0)$, R_{56} being the dispersive section strength, and J_m is the mth order Bessel function. Once the initial electron-beam properties, i.e., $\langle\gamma\rangle_0$ and σ_γ, are fixed, the bunching at different harmonics can be optimized by properly choosing the strength of the dispersive section, R_{56}. The relation (4) is valid under the assumption that only energy modulation (i.e., no bunching) is created inside the modulator. Such an approximation is well justified when considering the classical scheme. In the classical scheme, m cannot be large and is generally $m \leq 6$. Indeed, significant bunching at higher harmonics would degrade the quality of the electron bunch by increasing the beam energy spread $\Delta\gamma$ produced in the modulator. This would in turn result in a degradation of the amplification process in the radiator. The need to limit the growth of the energy spread prevents the possibility of reaching short wavelengths in a single modulator-dispersive section-radiator "cascade." For this reason, present designs of FEL's based on CHG rely on a series of two [13] or more [14] consecutive cascades in which the radiation generated by intermediate radiator(s) is used as a seed for the following modulator(s).

The method we propose relies on the possibility of creating substantial bunching at the fundamental wavelength and harmonics inside the modulator while limiting the energy-spread growth. The scheme is shown in Fig. 1(b). With respect to the classical configuration [see Fig. 1(a)], the modulator is subdivided in two undulator sections. Between the two sections there is a phase shifter, the role of which is to control the relative phase between the electron beam and the optical field provided by the external seed laser.

Equations (1)–(3) have been solved numerically. Simulations reported in the following are based on the realistic parameter set adopted for the design of the first

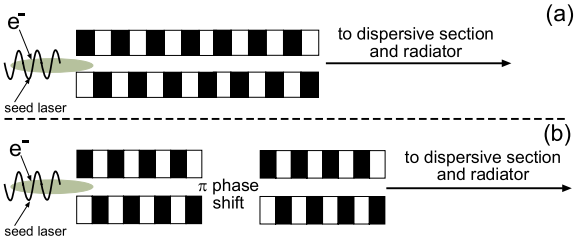

FIG. 1 (color online). Classical [8] and new proposed schemes for CHG using an external VUV seed laser.

stage of the FERMI@Elettra project [13]. Relevant parameters are $\langle\gamma\rangle_0 = 2349$ (electron-beam energy: 1.2 GeV), $\sigma_\gamma = 0.4$ (initial energy spread: 200 keV), $\rho = 7.5 \times 10^{-3}$. The two undulator modules are about 2 m long and the drift between them (where the phase shifter is located) is 0.5 m. The only important difference with respect to the FERMI@Elettra design is in the power of the seed laser, i.e., 100 MW for the FERMI case and about 10 GW for the double-modulator scheme. It is worth noting that, although the seed radiation density in the proposed scheme is larger than the one used for the standard FERMI and Bessy configurations, the condition for bunching creation [17] is still satisfied. The value of the laser intensity is the result of a careful optimization: it is low enough to be easily generated by presently available laser systems and strong enough to reduce both R_{56} and the length of the modulator, so that significant bunching is generated at high harmonics [see Eq. (5)]. Electrons are assumed to be initially unbunched, i.e., $b_h = 0$ $(h = 1, \ldots, m)$.

The limitation of the energy-spread growth is obtained by means of a prompt $\sim\pi$ shift of the electron-seed phase before the electron beam enters the second undulator section. The effect of the shift on the energy spread is shown in Fig. 2. In the first module ($z < 2$ m), the strong optical field induces a rapid coherent growth of the electron-beam energy spread, see Fig. 2(a). As shown in Fig. 2(c), such an energy modulation is essentially in phase with the optical field. After the $\sim\pi$ shift the energy modulation and the optical field get out of phase [see Fig. 2(d)]. In the second modulator section ($z > 2$ m) electrons with negative energy spread experience an accelerating field, while electrons with energy above resonance are instead decelerated. As a consequence, the energy spread at the exit of the second modulator is strongly reduced, see Figs. 2(a) and 2(e). A major difference to the standard configuration is that, while in the latter case only a low energy modulation is induced inside the (single) modulator, in the proposed scheme a significant bunching is already generated along the double modulator [see Fig. 2(b)]. Considering that the bunching evolution inside the undulator is given by $b_0(z) \propto \int_0^z \Delta\gamma(\xi)d\xi$, it is evident the advantage of a bump in energy spread (as in the double-modulator scheme), see Fig. 2(a).

After the end of the modulator electrons enter the dispersive section where the beam phase space is rotated and

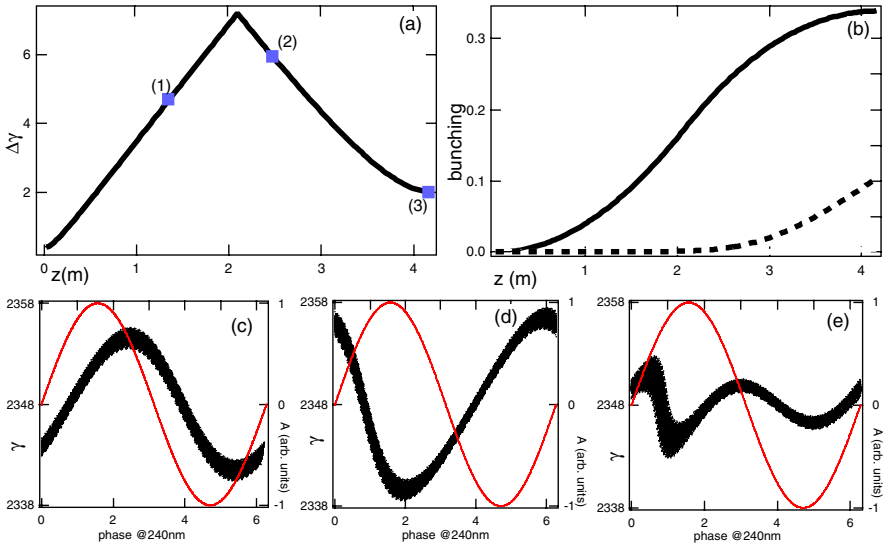

FIG. 2 (color online). Energy spread and bunching evolution inside the segmented modulator shown in Fig. 1(a): (a) energy spread vs z; (b) bunching vs z for the fundamental wavelength (continuous line) and for the 6th harmonic (dashed line); (c)–(e) electron-beam phase space at the end of the first module [point 1 in Fig. 2(a)], and at the beginning [point 2 in Fig. 2(a)] and at the end [point 3 in Fig. 2(a)] of the second one, respectively. The optical field profile is also reported. For the simulation use has been made of the parameters adopted for the design of the FERMI@Elettra FEL (see text).

the bunching at the desired harmonic optimized, see Fig. 3(a). Looking at the electron distribution versus phase, Fig. 3(b), one can see the bunching effect, due to which electrons concentrate around a given phase position. The width of the distribution, σ_ϕ, is related to the maximum harmonic number m at which a reasonable bunching is created. The condition to be fulfilled is $3\sigma_\phi < \pi/m$. The main contribution to σ_ϕ comes from the transformation of the initial incoherent energy spread, σ_γ, into phase spread. This occurs according to the following relation

$$\sigma\phi \simeq 2\pi \frac{\sigma_\gamma}{\langle\gamma\rangle_0}\left[2N + \frac{R_{56}}{\lambda}\right], \tag{5}$$

where N is the number of undulator periods. The first term at the right-hand side of Eq. (5) represents the energy-phase spread conversion occurring inside the modulator. The second term is the contribution to phase spread due to the dispersive section. Since significant bunching is already created inside the modulator, the needed value of the dispersive section strength, R_{56}, is a factor 4–5 smaller in the case of the double-modulator scheme. The need of a smaller R_{56} results in turn in a smaller σ_ϕ and, as a consequence, in a stronger bunching at higher harmonics with respect to the standard configuration. A Gaussian fit of the electron phase distribution at the exit of the dispersive section [dashed curve in Fig. 3(b)] gives $\sigma_\phi = 0.16$, which is slightly larger than the value predicted by Eq. (5). The additional contribution [not included in Eq. (5)] comes from the residual curvature in the electron-beam phase space when the beam is rotated in the dispersive section. Using the FERMI@Elettra parameter set, the value of σ_ϕ allows the existence of sufficient bunching up to $m \simeq 12$, as demonstrated in Fig. 3(c), where the electron distribution is plotted considering the 12th harmonic of the initial seeding signal at 240 nm.

These results are corroborated by the data shown in Fig. 4(a) (continuous line), where the maximum achievable bunching at different harmonics is plotted for the considered initial conditions. Figure 4(a) also shows the same curve for the standard method (dashed line). Such a curve has been calculated by optimizing Eq. (4) for the same electron-beam parameters and final induced energy spread. Assuming a bunching of 10% as the minimum required to get a good coherent/incoherent signal ratio, one can see that while the standard method allows effective harmonic generation at wavelengths not shorter than $\lambda/6$ (i.e., 40 nm), a factor of 2 can be easily gained by using the modified scheme.

The theoretical findings obtained using the simple 1D theoretical model (1)–(3) have been checked by means of the 3D numerical code Genesis, which properly takes into account light diffraction and transverse electron-beam dynamics. The significant enhancement of the system performance using the double-modulator scheme has been

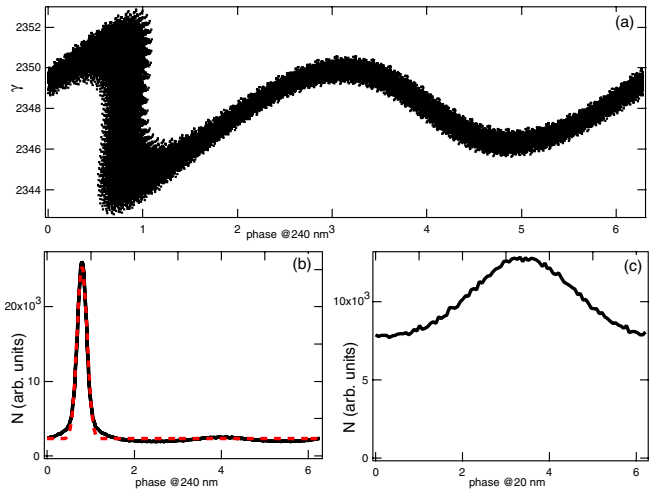

FIG. 3 (color online). (a) Electron-beam phase space at the exit of the dispersive section. (b) Histogram showing the electrons distribution along the phase at the fundamental wavelength (i.e., 240 nm). (c) Histogram showing the electrons distribution along the phase at the 12th harmonic of the fundamental wavelength (i.e., 20 nm).

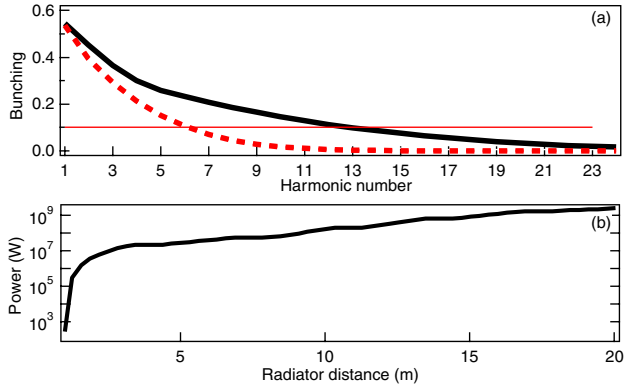

FIG. 4 (color online). (a) Bunching vs harmonic number at the exit of the dispersive section as obtained using the standard configuration (dashed line) and the double-modulator scheme (continuous line). (b) Peak power vs radiator distance as obtained using the numerical code Genesis. The input electron beam has been "prepared" with Genesis using the double-modulator scheme. Radiator is tuned at 20 nm, that is the twelfth harmonic of the seed laser. Additional input parameters: beam energy: 1.2 GeV, beam energy spread: 200 keV, beam emittance: 1.5 mm mrad, beam current: 1 kA, seed power: 10 GW, seed waist (inside modulator): 900 μm. The undulator is subdivided in six sections of 2.5 m separated by drifts of 0.5 m where the electron beam is refocused by means of alternate focusing quadrupoles (average beam dimensions inside undulator: 80 μm).

fully confirmed. In Fig. 4(b) is shown the peak power emitted along the radiator tuned at 20 nm. The strong initial bunching at the amplified wavelength is responsible for the initial steep quadratic growth. Power saturates above 1 GW after six undulator sections of 2.5 m.

Because of the strong bunching occurring in the modulator, the double-modulator scheme will be also less sensitive to the broadening of the FEL output bandwidth caused by any residual energy chirp in the electron-beam distribution. When electrons cross the dispersive section, a nonlinear variation of the beam energy profile is transformed into a broadening of the central wavelength. Such a broadening depends on the strength of the dispersive section according to the following relation: $\Delta\lambda = \lambda R_{56} d\gamma/(dz\langle\gamma\rangle_0)$. As already pointed out, in the double-modulator scheme, the value of R_{56} is significantly smaller than in the standard configuration. As a result, spectral broadening will be smaller as well and the output FEL pulse will be closer to the transform limit.

Up to this point, it has been shown that the proposed method can be used to significantly improve the performance of the classical single-cascade scheme. For this purpose, use has been made of the "conservative" set of parameters which are currently utilized for the design of the FERMI@Elettra FEL. However, the great potential of the double-undulator scheme can be better appreciated by assuming more "aggressive" (although still realistic) initial conditions. Consider Eq. (5): the way to further extend the accessible spectral region relies on the improvement of the phase resolution after the dispersive section. Such an improvement can be obtained by decreasing the relative energy spread $\sigma_\gamma/\langle\gamma\rangle_0$. Reducing the relative energy spread by a factor four with respect to the FERMI@Elettra case allows, for instance, to get significant bunching after the dispersive section at the 48th harmonic of the seed laser, that is 5 nm.

In conclusion, we have demonstrated a simple method allowing to significantly extend the spectral region covered by a single-cascade FEL. The main limitation to the quest for short wavelengths is represented by the relative beam incoherent energy spread. For realistic values of such a parameter the scheme we propose is able to reach wavelengths as short as few nm. The method is easy to implement and can be expected to have an impact on the realization of future facilities based on coherent harmonic generation using a single-pass free-electron laser.

The authors are grateful to W. M. Fawley for enlightening discussions.

[1] C. Pellegrini, Proceedings EPAC Conference 2006, http://accelconf.web.cern.ch/AccelConf/e06/PAPERS/FRYBPA01.PDF.
[2] J. R. Schneider, Proceedings FEL Conference 2006, http://accelconf.web.cern.ch/AccelConf/f06/PAPERS/MOBAU03.PDF .
[3] R. Bonifacio, C. Pellegrini, and L. Narducci, Opt. Commun. **50**, 373 (1984); K. J. Kim, Phys. Rev. Lett. **57**, 1871 (1986); D. A. Kirkpatrick *et al.*, Phys. Fluids B **1**, 1511 (1989); S. V. Milton, Phys. Rev. Lett. **85**, 988 (2000); J. Andruszhow, Phys. Rev. Lett. **85**, 3825 (2000); R. Brinkmann, Proceedings FEL Conference 2006, http://cern.ch/AccelConf/f06/TALKS/FRBAU01_TALK.PDF.
[4] J. Feldhaus *et al.*, Opt. Commun. **140**, 341 (1997); Z. Huang and R. D. Ruth, Phys. Rev. Lett. **96**, 144801 (2006).
[5] R. Coisson and F. De Martini, *Physics of Quantum Electronics* (Addison-Wesley, Reading, MA, 1982), Vol. 9, p. 939.
[6] B. Girard *et al.*, Phys. Rev. Lett. **53**, 2405 (1984).
[7] R. Bonifacio *et al.*, Nucl. Instrum. Methods Phys. Res., Sect. A **296**, 787 (1990).
[8] L. H. Yu, Phys. Rev. A **44**, 5178 (1991).
[9] H. P. Freund, S. G. Biedron, and S. V. Milton, IEEE J. Quantum Electron. **36**, 275 (2000).
[10] S. G. Biedron *et al.*, Nucl. Instrum. Methods Phys. Res., Sect. A **475**, 118 (2001).
[11] A. Doyuran *et al.*, Phys. Rev. Lett. **86**, 5902 (2001).
[12] L. H. Yu *et al.*, Phys. Rev. Lett. **91**, 074801 (2003).
[13] G. Bocchetta *et al.*, Proceedings FEL Conference 2006, http://accelconf.web.cern.ch/AccelConf/f06/PAPERS/MOPPH054.PDF.
[14] A. Meseck *et al.*, Proceedings FEL Conference 2006, http://accelconf.web.cern.ch/AccelConf/f06/PAPERS/MOCAU01.PDF .
[15] W. B. Colson, Phys. Lett. **59A**, 187 (1976); R. Bonifacio *et al.*, Opt. Commun. **50**, 373 (1984).
[16] S. Reiche, Nucl. Instrum. Methods Phys. Res., Sect. A **429**, 243 (1999).
[17] H. K. Avetissian *et al.*, Phys. Lett. **66A**, 161 (1978).